

An Analysis of Two Nonlinear Observers in the Presence of Noise

Nitin Patel, Christopher Edwards, Sarah K Spurgeon

Abstract—This paper compares two nonlinear observers designed to estimate a road condition parameter. Both schemes assume only wheel angular velocity is measured and are based on a quarter vehicle model. A stability analysis is made of the estimation scheme in the presence of noise associated with the wheel angular velocity measurement in an effort to explain the results from the simulations.

I. INTRODUCTION

Recently, the automobile industry has concentrated on developing intelligent systems for dynamic performance and safety improvements. Many new features on automotive vehicles are available such as anti-lock brake systems (ABS), traction control systems (TCS), adaptive cruise control (ACC), active yaw control, active suspension systems, engine management systems (EMS) and vehicle management systems which all incorporate advanced data acquisition systems. These systems rely on the physical parameters of the vehicle and information about the environmental conditions in which it is operating. It is important to note that the adhesion between the tyre and road (the friction force) is less for decreasing velocities than for increasing velocities. Therefore, a good estimate of the road/tyre friction coefficient is an important basis for many of the control systems developed to improve safety in an emergency braking situation. Various methods have been developed to predict tyre/road friction – for example [1], [3]-[7], [9], [12]. Most of these schemes make use of the available data from wheel speed sensors to compute an estimate of the tyre/road friction.

Alvarez *et al.* [1] proposed a friction estimation method which uses measurements of wheel angular velocity and longitudinal vehicle acceleration. From the measurement of wheel angular velocity, they propose numerically computing wheel angular acceleration. These three signals are then used in the estimation of the friction coefficients and in the brake input control law. Most of the other schemes in the literature assume that only information about angular velocity is known. Yi *et al.* [12] use a LuGre friction model [2] and investigate nonlinear adaptive observers based on measurements of wheel speed. More recently, a sliding mode based scheme has been proposed [8] in which analytical expression for the gains are given – parameterized by a single scalar which reflects the rate at which sliding is obtained. During sliding, the equivalent output estimation error is used to estimate a road surface parameter which characterizes the surface on which the vehicle is moving. As in all the other comparable schemes [1], [3]-[12], it is

assumed that the parameters of the vehicle including the mass, effective wheel radius and moments of inertia are fixed and known. None of the papers [1], [3]-[12] consider the effect of noise on the estimation schemes. In this paper a stability analysis is made of the estimation scheme in the presence of noise associated with the wheel angular velocity measurement. A comparison of the results between the sliding mode observer in [8] and the adaptive observer in [12] is shown. An analysis is made of both schemes to explain the results from the simulations.

II. TYRE/ROAD FRICTION AND VEHICLE MODELLING

In many friction models, the environmental conditions in which the vehicle operates are taken into account by means of a ‘road surface condition’ parameter [1], [3]-[12]. Consider the dynamic LuGre friction model from [3] together with a simple model of the vehicle dynamics:

$$\dot{z}_f = -v_r - \theta \frac{\sigma_0 |v_r|}{h(v_r)} z_f \quad (1)$$

$$J\dot{\omega} = -rF_x - k_b P_b \quad (2)$$

$$m\dot{v} = 4F_x - F_{av} \quad (3)$$

where v is the longitudinal velocity of the vehicle, ω is angular wheel speed, $v_r = v - r\omega$ is the relative velocity and z_f is an internal frictional state. From [3], the friction force F_x produced by the tyre/road contact is given by

$$F_x = F_n(\sigma_0 z_f + \sigma_1 \dot{z}_f - \sigma_2 v_r) \quad (4)$$

where σ_0 is the stiffness coefficient, σ_1 is the damping coefficient, and σ_2 is the viscous relative damping coefficient. The scalar function

$$h(v_r) := \mu_c + (\mu_s - \mu_c) e^{-|\frac{v_r}{v_s}|^{\frac{1}{2}}} \quad (5)$$

where v_s is Stribeck relative velocity, μ_s is the normalized static friction coefficient and μ_c is the normalized Coulomb friction coefficient. The parameter θ in (1) captures changes in the road characteristics: typically, $\theta = 1$ represents dry, $\theta = 2.5$ represents wet and $\theta = 4$ represents icy road conditions. The scalar J is the moment of inertia of the wheel, m is the total mass of the vehicle, F_{av} represents the aerodynamic force, k_b the brake system gain and P_b is the actual applied braking pressure (the control variable).

Here it will be assumed that the vehicle is travelling on a flat road and the load associated with the mass of the vehicle is equally distributed about each wheel which means $F_n = mg/4$ where g is the gravity constant. As in [12], assume $F_{av} = \sigma_v mgv$ where σ_v is a rolling resistance coefficient. Two different observer schemes will be considered: the sliding mode scheme proposed in [8] and the adaptive observer from [12].

N. Patel, C. Edwards and S.K. Spurgeon are with the Control and Instrumentation Research Group in the Department of Engineering, University of Leicester, University Road, Leicester, LE1 7RH, UK.

III. A SLIDING MODE OBSERVER

Choosing as states $x_1 = z_f$, $x_2 = v$ and $x_3 = r\omega - v$, a sliding mode observer [5], [10], [11] will be described based on the assumption that only the angular velocity ω is available (which can be measured easily). For the purpose of observer design it is convenient to split the state-space equations associated with (1)- (3) into linear and nonlinear components in a Lur'e type form:

$$\dot{x}(t) = Ax(t) + Bu(t) + D\theta x_1(t)f(x_3) \quad (6)$$

where the control signal $u(t) = P_b(t)$ and

$$A = \begin{bmatrix} 0 & 0 & 1 \\ g\sigma_0 & -g\sigma_v & g(\sigma_1 + \sigma_2) \\ q\sigma_0 & g\sigma_v & q(\sigma_1 + \sigma_2) \end{bmatrix} \quad B = \begin{bmatrix} 0 \\ 0 \\ -\frac{rk_b}{J} \end{bmatrix} \quad (7)$$

The distribution matrix through which the nonlinear term operates is

$$D = \begin{bmatrix} -1 \\ -g\sigma_1 \\ -q\sigma_1 \end{bmatrix} \quad (8)$$

In these matrices the aggregate parameter

$$q := -(g + F_n r^2 / J) \quad (9)$$

has been used. Since it is assumed that only angular wheel speed ω is measured, the output distribution matrix

$$C = \begin{bmatrix} 0 & \frac{1}{r} & \frac{1}{r} \end{bmatrix} \quad (10)$$

A. A Sliding Mode Observer

The following sliding mode observer was proposed in [8]

$$\dot{\hat{x}}(t) = A\hat{x}(t) + Bu(t) + G_l e_y + D\nu \quad (11)$$

where $G_l = \text{col}(g_1, g_2, g_3)$ with g_1, g_2 and g_3 scalars; and $\nu = k \text{sgn}(e_y)$ where k is a scalar gain. The sliding mode observer guarantees $e_y = 0$ in finite time where $e_y = \omega - \hat{\omega}$, and $e := x - \hat{x} \rightarrow 0$ as $t \rightarrow \infty$ despite the nonlinear friction terms which have been ignored in (11). It is shown in [8] that if

$$\bar{g}_1 = r + (g + \frac{\alpha}{\sigma_1}) \frac{J}{F_n r} \quad (12)$$

$$\bar{g}_2 = g(\alpha + g\bar{\sigma} - \frac{\sigma_0}{\sigma_1}) \frac{J}{F_n r} + gr(\sigma_1 + \sigma_2) \quad (13)$$

$$\bar{g}_3 = (\sigma_1 + \sigma_2)q - \frac{\sigma_w}{J} + \frac{\sigma_0}{\sigma_1} - \alpha \quad (14)$$

where $\bar{\sigma} = \sigma_v + \sigma_1 + \sigma_2$ and α is a negative scalar then

$$G_l = \begin{bmatrix} \bar{g}_1 \\ \bar{g}_2 \\ r\bar{g}_3 - \bar{g}_2 \end{bmatrix} \quad (15)$$

is an appropriate choice of gain in (11). *If the wheel speed can be measured perfectly* then the dynamics for the error system can be obtained from (6) and (11) as

$$\dot{e} = (A - G_l C)e + D(\theta f(x_3)x_1 - \nu) \quad (16)$$

Proposition 1 [8]: *The state estimation error system (16) is quadratically stable for large enough k . Furthermore in*

a domain of the origin, a sliding motion takes place on $\mathcal{S} = \{e : Ce = 0\}$ in finite time. ■

As argued in [8] when $e \rightarrow 0$, the expression for the equivalent output error injection signal ν_{eq} , necessary to maintain a sliding motion in the state estimation error space, becomes

$$\nu_{eq} = \theta f(x_3)x_1 \quad (17)$$

Equation (17) indicates that the expression

$$\hat{\theta} = \frac{\nu_{eq}}{f(\hat{x}_3)\hat{x}_1} \quad (18)$$

can be used as an estimate for the parameter θ during the sliding motion. Since $\hat{x}_1 \rightarrow x_1$ and $\hat{x}_3 \rightarrow x_3$ it follows $f(\hat{x}_3)\hat{x}_1 \rightarrow f(x_3)x_1$ and so $\hat{\theta} \rightarrow \theta$. Notice (17) is only valid when $\hat{x}_1 \neq 0$ and $\hat{x}_3 \neq 0$ since $f(\hat{x}_3) > 0$ if $x_3 \neq 0$ by definition.

B. Stability Analysis

Suppose the measurement is corrupted with noise so that $y = \omega + n$, where $n \in \mathbb{R}$ is assumed to be differentiable and bounded. Define $e_1 = x_1 - \hat{x}_1$, $e_2 = x_2 - \hat{x}_2$ and $e_3 = x_3 - \hat{x}_3$. In the presence of noise associated with measurement of angular velocity ω , the output error

$$e_y = Ce + n \quad (19)$$

and the errors e_1, e_2 and e_3 satisfy

$$\dot{e}_1 = e_3 - \theta f(x_3)x_1 - k_1 e_y + \nu \quad (20)$$

$$\dot{e}_2 = g(\sigma_0 e_1 + \sigma_1(e_3 - \theta f(x_3)x_1) + \sigma_2 e_3) - \sigma_v g e_2 - k_2 e_y + g\sigma_1 \nu \quad (21)$$

$$\dot{e}_3 = q(\sigma_0 e_1 + \sigma_1(e_3 - \theta f(x_3)x_1) + \sigma_2 e_3) - \frac{\sigma_\omega}{J}(e_2 + e_3) + \sigma_v g e_2 - k_3 e_y + q\sigma_1 \nu \quad (22)$$

During sliding $e_y = 0$ and

$$\dot{e}_y = \frac{\dot{e}_2 + \dot{e}_3}{r} + \dot{n} = 0 \quad (23)$$

Substituting for \dot{e}_2 and \dot{e}_3 from equation (21) and (22) and taking into account that $e_y = 0$ means the equivalent output error injection necessary to maintain sliding is given by

$$\nu_{eq} = -\frac{1}{\sigma_1}(\sigma_0 e_1 + \sigma_1(e_3 - \theta f(x_3)x_1) + \sigma_2 e_3) - \frac{r\sigma_\omega}{(g+q)J\sigma_1}n - \frac{r}{(g+q)\sigma_1}\dot{n} \quad (24)$$

Substituting the value of ν_{eq} from (24) into equation (20) gives the expression

$$\dot{e}_1 = \frac{\sigma_0}{\sigma_1}e_1 - \frac{\sigma_2}{\sigma_1}e_3 - \frac{r\sigma_\omega}{(g+q)J\sigma_1}n - \frac{r}{(g+q)\sigma_1}\dot{n} \quad (25)$$

Define a new variable

$$\tilde{e}_1 := e_1 + \frac{r}{(g+q)\sigma_1}n \quad (26)$$

then using the expression for \dot{e}_1 from (25) in the above equation gives

$$\dot{e}_1 = -\frac{\sigma_0}{\sigma_1}e_1 - \frac{\sigma_2}{\sigma_1}e_3 - \frac{r\sigma_\omega}{(g+q)J\sigma_1}n \quad (27)$$

Substituting for ν_{eq} from (24) into (22) and noting that during sliding $e_y = 0$, which means $e_2 = -e_3 - rn$, it follows that

$$\dot{e}_3 = -\sigma_v g e_3 + \left(\frac{\sigma_\omega r}{J} - \frac{r\sigma_\omega q}{J(g+q)} - \sigma_v g r \right) n - \frac{r}{(g+q)} q \dot{n} \quad (28)$$

Define

$$\tilde{e}_3 = e_3 + \frac{r}{(g+q)} q n \quad (29)$$

which implies from (28) that

$$\dot{\tilde{e}}_3 = -\sigma_v g e_3 + \left(\frac{\sigma_\omega g r}{J(g+q)} - \sigma_v g r \right) n \quad (30)$$

Using the expressions in equations (26) and (29), equation (27) can be re-written as

$$\dot{\tilde{e}}_1 = -\frac{\sigma_0}{\sigma_1}\tilde{e}_1 - \frac{\sigma_2}{\sigma_1}\tilde{e}_3 + \frac{r}{\sigma_1(g+q)} \left(\frac{\sigma_0}{\sigma_1} + \sigma_2 q - \frac{\sigma_\omega}{J} \right) n \quad (31)$$

and after some algebra, equation (30) can be re-written as

$$\dot{\tilde{e}}_3 = -\sigma_v g \tilde{e}_3 + \frac{4}{mr} (Jg\sigma_v - \sigma_\omega) n \quad (32)$$

In order to obtain an expression for the equivalent injection ν_{eq} in practice, the signal ν is passed through a low-pass filter. From equation (24) if a first order low pass filter is employed to obtain ν_f , then

$$\dot{\nu}_f + \tau \nu_f = -\frac{\tau}{\sigma_1} (\sigma_0 e_1 + (\sigma_1 (e_3 - \theta f(x_3) x_1) + \sigma_2 e_3) - \frac{\tau r \sigma_\omega}{(g+q)J\sigma_1} n - \frac{\tau r}{(g+q)\sigma_1} n) \quad (33)$$

where τ is the time constant of the filter. Define

$$\tilde{\nu}_f := \nu_f + \frac{r\tau}{\sigma_1(g+q)} n \quad (34)$$

then from (34) and (33), and using the expressions in equations (26) and (29), equation (33) becomes

$$\dot{\tilde{\nu}}_f = -\tau \tilde{\nu}_f - \frac{\sigma_0}{\sigma_1} \tau \tilde{e}_1 - \tau \left(1 + \frac{\sigma_2}{\sigma_1} \right) \tilde{e}_3 + \tau \theta f(x_3) x_1 + \frac{r\tau}{\sigma_1(g+q)} \zeta n \quad (35)$$

where $\zeta := \left(\frac{\sigma_0}{\sigma_1} + q\sigma_1 + \sigma_2 q + \tau - \frac{\sigma_\omega}{J} \right)$.

In the case when $n \equiv 0$, i.e. the measurements are noise free, from (27) and (30) the $(\tilde{e}_1, \tilde{e}_3)$ subsystem is asymptotically stable and $\tilde{e}_1 \rightarrow 0$ and $\tilde{e}_3 \rightarrow 0$. When $e_1, e_3 = 0$, equation (35) becomes

$$\dot{\tilde{\nu}}_f = -\tau \tilde{\nu}_f + \tau \theta f(x_3) x_1 \quad (36)$$

and $\tilde{\nu}_f \rightarrow \theta f(x_3) x_1 \Rightarrow \nu_f \rightarrow \theta f(x_3) x_1$

Now suppose that $n \neq 0$ but is predominantly composed of high frequency components and satisfies

$$\dot{n} + \kappa n = \xi \quad (37)$$

for some differentiable signal $\xi \in \mathbb{R}$ and some scalar κ which is related to the frequency range of the noise. Define

$$\tilde{n} = n - \xi \Rightarrow \dot{\tilde{n}} - \kappa(\tilde{n} + \xi) \quad (38)$$

then from equations (26), (29) and (34):

$$\begin{bmatrix} \dot{e}_1 \\ \dot{e}_3 \\ \dot{\nu}_f \end{bmatrix} = \underbrace{\begin{bmatrix} 1 & 0 & 0 & -\frac{r}{\sigma_1(g+q)} \\ 0 & 1 & 0 & -\frac{r}{g+q} \\ 0 & 0 & 1 & -\frac{r}{\sigma_1(g+q)}\tau \end{bmatrix}}_{C_\tau} \begin{bmatrix} \tilde{e}_1 \\ \tilde{e}_3 \\ \tilde{\nu}_f \end{bmatrix} - \underbrace{\begin{bmatrix} \frac{r}{\sigma_1(g+q)} \\ \frac{r}{g+q} \\ \frac{r}{\sigma_1(g+q)}\tau \end{bmatrix}}_{D_\tau} \xi \quad (39)$$

Similarly equations (31), (32), (35) and (38) can be represented as

$$\begin{bmatrix} \dot{\tilde{e}}_1 \\ \dot{\tilde{e}}_3 \\ \dot{\tilde{\nu}}_f \\ \dot{\tilde{n}} \end{bmatrix} = \underbrace{\begin{bmatrix} -\frac{\sigma_0}{\sigma_1} & -\frac{\sigma_2}{\sigma_1} & 0 & \vartheta \\ 0 & -\sigma_v g & 0 & \frac{4}{mr}(Jg\sigma_v - \sigma_\omega) \\ -\frac{\sigma_0}{\sigma_1}\tau & -(1 + \frac{\sigma_2}{\sigma_1})\tau & -\tau & \frac{r\tau}{\sigma_1(g+q)}\zeta \\ 0 & 0 & 0 & -\kappa \end{bmatrix}}_{A_\tau} \begin{bmatrix} \tilde{e}_1 \\ \tilde{e}_3 \\ \tilde{\nu}_f \\ \tilde{n} \end{bmatrix} + \begin{bmatrix} 0 \\ 0 \\ \tau \\ 0 \end{bmatrix} \theta f(x_3) x_1 + \underbrace{\begin{bmatrix} \vartheta \\ \frac{4}{mr}(Jg\sigma_v - \sigma_\omega) \\ \frac{r\tau}{\sigma_1(g+q)}\zeta \\ -\kappa \end{bmatrix}}_{B_\tau} \xi \quad (40)$$

where $\vartheta = \frac{r}{\sigma_1(g+q)} \left(\frac{\sigma_0}{\sigma_1} + \sigma_2 q - \frac{\sigma_\omega}{J} \right)$. The linear system $(A_\tau, B_\tau, C_\tau, D_\tau)$ defined in (39)-(40) governs the effect of the noise on the reduced order state observation errors e_1 and e_3 and the filtered equivalent output error injection signal. For a given noise frequency value (associated with the scalar κ) and a selected value of the cutoff frequency τ in the filter used to extract the equivalent injection ν_f , the system $(A_\tau, B_\tau, C_\tau, D_\tau)$ is totally determined by the model parameters. The properties of the system $(A_\tau, B_\tau, C_\tau, D_\tau)$ will be explored with respect to changes in the choice of τ i.e. the choice of filter to extract the equivalent output error injection. In this paper the \mathcal{L}_2 gain between ξ and (e_1, e_3, ν_f) will be used as the measure. Since $(A_\tau, B_\tau, C_\tau, D_\tau)$ represents the mapping between ξ and (e_1, e_3, ν_f) , the \mathcal{H}_∞ norm of $(A_\tau, B_\tau, C_\tau, D_\tau)$ is the \mathcal{L}_2 gain in this situation.

IV. ADAPTIVE OBSERVER

In [12] an adaptive observer was proposed based on a different choice of state variable, although the underlying system model is the one given in subsystem (1) - (5).

Specifically, let $z = \text{col}(\sigma_0 z_f, v, v - r\omega)$, and write the vehicle model as

$$\dot{z} = A_a z + B_a u + D_a \theta f(z_3) z_1 \quad (41)$$

$$y = C_a z + n \quad (42)$$

where $f(z_3) := \frac{z_3}{h(z_3)}$ where $h(\cdot)$ is defined in (5). Again n represents measurement noise. In [12] the following adaptive observer was proposed

$$\dot{\hat{z}} = A_a \hat{z} + B_a u + D_a \hat{\theta} f(\hat{z}_3) \hat{z}_1 + L e_y + D_a \Upsilon(e_y) \quad (43)$$

where $e_y = y - C_a \hat{z}$. The matrix $L \in \mathbb{R}^3$ is a design gain and the nonlinear output error injection term

$$\Upsilon(e_y) = \frac{\rho_4}{4} \left(\frac{\rho_3 r}{\rho_2} \right)^2 \hat{z}_1^2 e_y \quad (44)$$

where ρ_2, ρ_3 and ρ_4 are appropriately chosen parameters [12]. The estimate of θ , denoted by $\hat{\theta}$, is obtained using the following adaptive scheme

$$\dot{\hat{\theta}} = 2\gamma f(\hat{z}_3) \hat{z}_1 e_y \quad (45)$$

where γ is a positive design scalar.

Define $\tilde{z} = z - \hat{z}$. The error dynamics for the system is given by

$$\dot{\tilde{z}} = (A_a - LC_a) \tilde{z} + D_a \left(\theta \psi(z) - \hat{\theta} \psi(\hat{z}) \right) - D_a \Upsilon(e_y) \quad (46)$$

where $\psi(z) := f(z_3) z_1$ and $\psi(\hat{z}) = f(\hat{z}_3) \hat{z}_1$. Consider a Lyapunov function candidate

$$V = \tilde{z}^T P_a \tilde{z} + \frac{1}{2\gamma} \tilde{\theta}^2 \quad (47)$$

where P_a is a symmetric positive definite matrix and the estimation error $\tilde{\theta} = \theta - \hat{\theta}$. In [12], the following assumptions are made: there exists an L and a symmetric positive definite matrix P_a such that

$$(A_a - LC_a)^T P_a + P_a (A_a - LC_a) + (\rho_1^2 + \rho_4) I < 0 \quad (48)$$

where ρ_1 is a positive scalar, and

$$P_a D_a = C_a^T \quad (49)$$

In the presence of noise, $e_y = \tilde{y} + n$ it can be shown using arguments similar to those in [12] that

$$\begin{aligned} \dot{V} \leq & -\rho_1^2 \|\tilde{z}\|^2 - \frac{\rho_4}{2} \left(\tilde{z}_3 - \frac{\rho_3 r}{\rho_2} \hat{z}_1 \tilde{y} \right)^2 \\ & + \frac{\rho_4}{2} \left(\frac{\rho_3 r}{\rho_2} \right)^2 \hat{z}_1^2 \tilde{y} n + 2\tilde{\theta} \psi(\hat{z}) n \end{aligned} \quad (50)$$

In the absence of noise, $n \equiv 0$ and so

$$\dot{V} \leq -\rho_1^2 \|\tilde{z}\|^2 - \frac{\rho_4}{2} \left(\tilde{z}_3 - \frac{\rho_3 r}{\rho_2} \hat{z}_1 \tilde{y} \right)^2 \leq 0 \quad (51)$$

and so asymptotic convergence of $\tilde{z} \rightarrow 0$ can be shown. Furthermore using a persistence of excitation type argument, if θ is fixed, $\tilde{\theta} \rightarrow 0$ and so $\hat{\theta} \rightarrow \theta$. However, equation (50) shows that in the presence of measurement noise associated with the angular velocity ω , Lyapunov stability is not guaranteed.

V. RESULTS

In this section the results from both observers will be compared. The friction and vehicle parameters used to produce the results are: $v_s = 10\text{m/s}$, $\sigma_0 = 100\text{m}^{-1}$, $\sigma_1 = 0.7\text{s/m}$, $\sigma_2 = 0.011\text{s/m}$, $\mu_c = 0.35$, $\mu_s = 0.5$ and $r = 0.323\text{m}$, $J = 2.603\text{kg/m}^2$, $m = 1701\text{kg}$, $\sigma_v = 0.005$ and $k_b = 0.9$. The estimated value of θ obtained from (18) is filtered using a 1st order low pass filter. This is in keeping with the estimation of ν_{eq} from ν as the low frequency components of the switched injection signal. To generate a fair comparison, the value of θ obtained from (45) is filtered using the same filter.

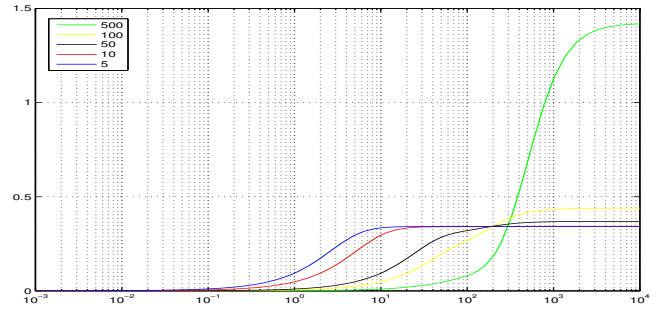


Fig. 1. Bode plot with high pass filter.

Figure 1 shows a plot of the maximum singular values of the frequency responses of the systems given by $(A_\tau, B_\tau, C_\tau, D_\tau)$ for a range of values of τ between 5 and 500. In the plot, the cut-off frequency κ associated with the noise equation in (37) is $\kappa = 5$. It can be seen that $\tau = 100$ is a good choice of cut-off frequency for the filter to extract the equivalent control in (33). For $\tau > 100$ the singular values become high at high frequency indicating significant transmission of noise onto the estimates.

In the following simulations the gain associated with the nonlinear injection term for the sliding mode observer is $k = 50$ whilst $g_1 = 0.3433$, $g_2 = -0.3118$ and $g_3 = 16.5009$. These values have been calculated according to the formulae in (12)-(14) and guarantee a sliding motion will take place in finite time. For the adaptive observer the gain $L = [-400 \quad -60 \quad -500]$ has been used as given in [12]. The value for $\kappa(e_y)$ in the adaptive observer was obtained from (44) taking $\lambda_{max} = 0.4$, $\theta_{max} = 4$ and $v_{max} = 30$. The adaptation gain was selected as $\gamma = 200$ as given in [12]. The brake input signal was assumed to be available and for both observers the same brake input was used during the simulations which results in a sharp decrease in longitudinal velocity from an initial longitudinal speed of 30m/s .

Figures 2 - 4 show the performance of the observers when there is noise on the measurement of angular velocity ω . Figure 2 shows the plant states and estimated states using the sliding mode observer and Figure 3 shows the plant states and the estimated states using the adaptive observer. There is visible degradation in the estimate of v_r in Figure 3.

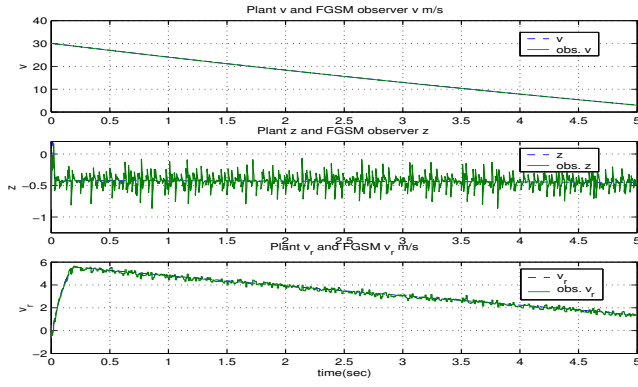


Fig. 2. States and estimated states using the sliding mode observer.

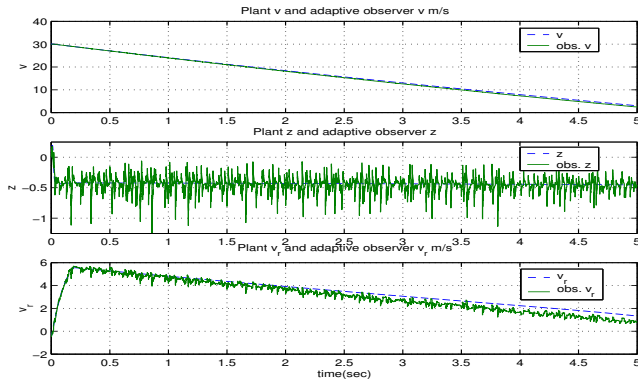


Fig. 3. States and estimated states using the adaptive observer.

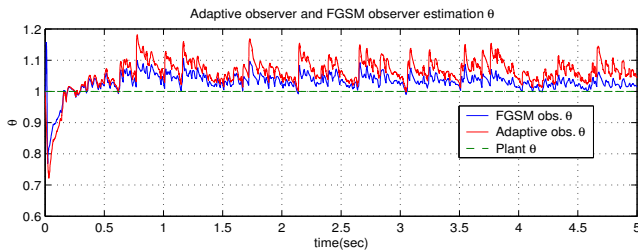


Fig. 4. Comparison of estimated θ .

Figure 4 shows the plant θ and the estimate $\hat{\theta}$ using the sliding mode observer and the adaptive observer. The figure shows the sliding mode observer gives better performance.

Figures 5 - 7 show the performance of the observers in the presence of varying road conditions $1 \leq \theta \leq 4$ with noise on the measurement of angular velocity ω . Figure 5 shows the plant states and the estimated states using the sliding mode observer. Figure 6 shows the plant states and the estimated states using the adaptive observer. It can be seen in Figure 6 that the adaptive observer estimates 'collapse' at around 5 seconds. Figure 7 shows the plant θ and the estimate $\hat{\theta}$ using the sliding mode observer and Figure 8 shows the plant θ and the estimate $\hat{\theta}$ using the adaptive observer. As expected from the poor levels of state estimation, the observer struggles to estimate θ correctly.

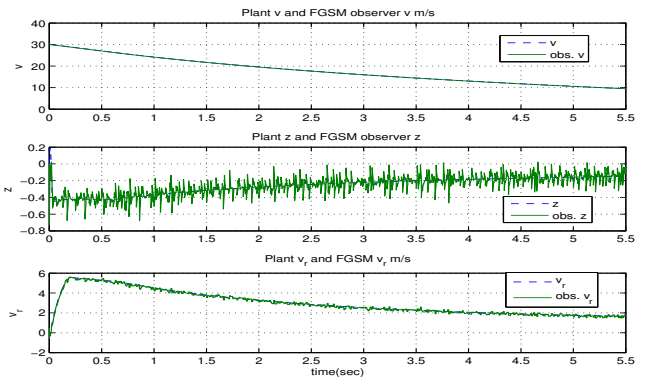


Fig. 5. States and estimated states using the sliding mode observer.

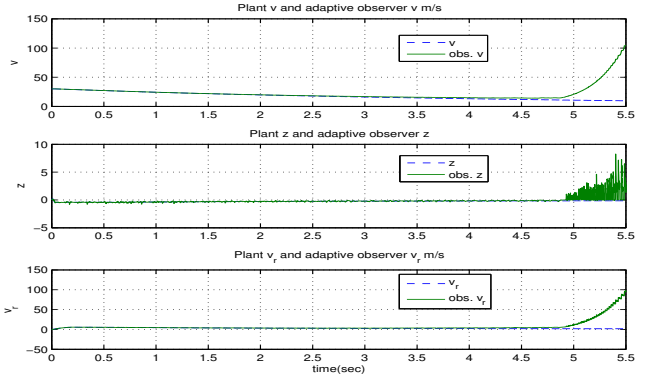


Fig. 6. States and estimated states using the adaptive observer.

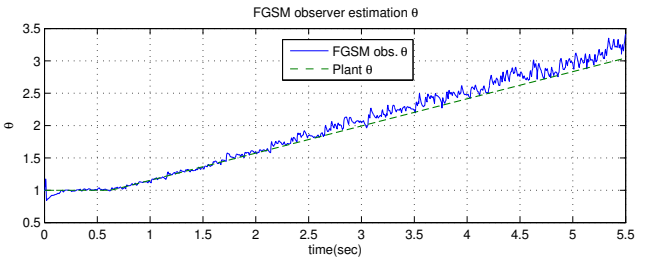


Fig. 7. Comparison of estimated θ .

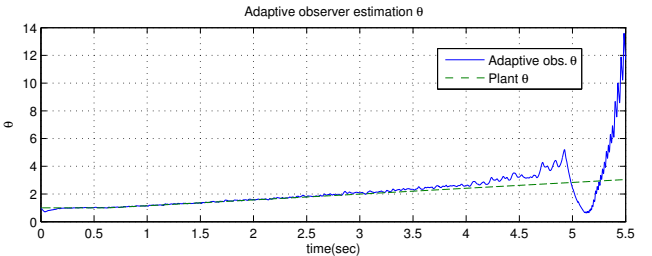


Fig. 8. Comparison of estimated θ .

The breakdown in the performance of the adaptive observer has motivated a redesign of the observer gain L from the original paper [12]. In the remaining simulations

$$L = [-400 \quad 60 \quad -500]$$

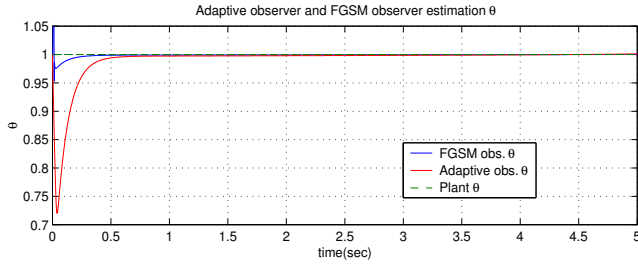


Fig. 9. Comparison of estimated θ .

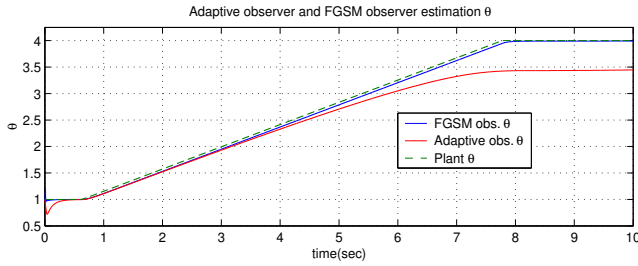


Fig. 10. Comparison of estimated θ .

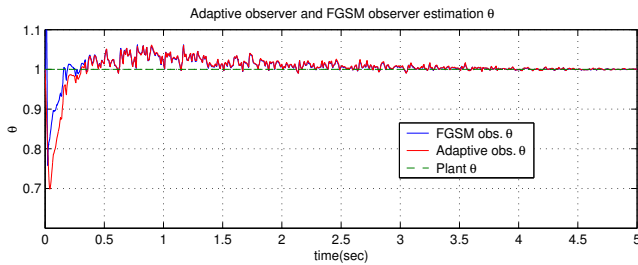


Fig. 11. Comparison of estimated θ .

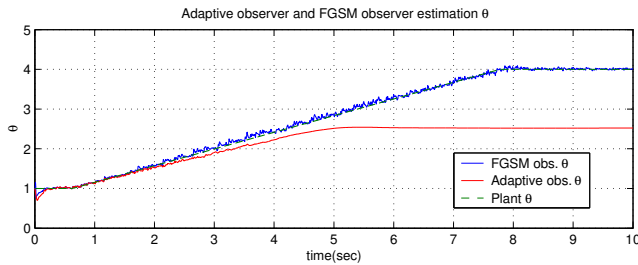


Fig. 12. Comparison of estimated θ .

has been chosen. Figure 9 shows the plot of the estimate of $\hat{\theta}$ when plant $\theta = 1$ using the sliding mode observer and the adaptive observer. From the figure both observers now show a similar performance level after an initial transient. Figure 10 shows the plot of the estimate of $\hat{\theta}$ when $1 \leq \theta \leq 4$ using the sliding mode observer and the adaptive observer. From Figure 10 it is clear that the adaptive observer underestimates θ . Figure 11 shows the plot of the estimate $\hat{\theta}$ using the sliding mode observer and the adaptive observer, when $\theta = 1$ and there is noise on the measurement of angular velocity ω . From the figure both

observers show similar performance levels. Figure 12 shows a plot of the estimate of $\hat{\theta}$ when $1 \leq \theta \leq 4$ when there is noise on the measurement of angular velocity ω . From the figure, the adaptive observer again underestimates θ (and the estimate is worse than in the noise free case).

VI. CONCLUSION

This paper has considered a comparative study of a sliding mode observer and an adaptive observer during deceleration in a braking manoeuvre. The effect of noise on the angular velocity measurement has been explored. Previously, in the literature neither of the schemes has been formally analyzed in this situation. The analysis, supported by simulation results, suggests that the sliding mode scheme is more robust than its adaptive counterpart. In certain conditions, the tracking performance of the adaptive observer in terms of both state estimation and estimation of the road condition parameter has been completely lost. Whilst noise degrades the performance of the sliding mode observer, in all the simulations, stability has been retained and a more robust reconstruction of θ has been obtained.

REFERENCES

- [1] L. Alvarez, J. Yi, R. Horowitz and L. Olmos. Dynamic Friction Model-Based Tyre/Road Friction Estimation and Emergency Braking Control. *Trans. of the ASME on Journal of Dynamic Systems, Measurement and Control*, March 2005.
- [2] C. Canudas de Wit, H. Olsson, K.J. Åström and P. Lischinsky. A new model for control of systems with friction. *IEEE Trans. on Automatic Control*, pages 419–425, 1995.
- [3] C. Canudas-de-Wit, P. Tsiotras, X. Claeys, J. Yi and R. Horowitz, *Friction Tyre/Road Modeling, Estimation and Optimal Braking Control in Nonlinear and Hybrid Systems in Automotive Control*, R. Johansson and A. Rantzer (editors). Springer-Verlag, London, UK, 2003.
- [4] S. Drakunov, U. Ozguner, P. Dix and B. Ashrafi. ABS control using optimum search via sliding modes. *IEEE Trans. on Control System Technology*, 3:79–83, 1995.
- [5] S. Drakunov and V.I. Utkin. Sliding mode observers: tutorial. In *Proc. of 34th IEEE CDC*, pages 3376–3378, 1995.
- [6] F. Gustafsson. Slip-based tyre-road friction estimation. *Automatica*, pages 1087–1099, 1997.
- [7] U. Kiencke. Real-time estimation of adhesion characteristic between tyre and road. In *Proceedings of the IFAC World Congress*, 1993.
- [8] N. Patel, C. Edwards and S.K. Spurgeon. A sliding mode observer for tyre friction estimation during braking. *Proceeding of the American Control Conference, Minneapolis*, pages 5867–5872 June 2006.
- [9] L.R. Ray. Nonlinear tyre force estimation and road friction identification - simulation and experiments. *Automatica*, 33:1819–1833, 1997.
- [10] V. I. Utkin. *Sliding Modes in Control Optimization*. Springer-Verlag, Berlin, 1992.
- [11] B. Walcott and S. Žak. State observation of nonlinear uncertain dynamical systems. *IEEE Trans. on Automatic Control*, Vol. AC-32, No.2, pp. 166–170, 1987.
- [12] J. Yi, L. Alvarez, X. Claeys and R. Horowitz. Emergency braking control with an observer-based dynamic tyre/road friction model and wheel angular velocity measurement. *Vehicle System Dynamics*, Vol.39, No.2:81–97, 2003.